

Internal photoemission spectroscopy for a PtSi/*p*-type Si Schottky-barrier diode

K. Konuma and Y. Asano

Microelectronics Research Laboratories, NEC Corporation, 1120 Shimokuzawa, Sagamihara, Kanagawa 229, Japan

K. Hirose

ULSI Device Development Laboratories, NEC Corporation, 1120 Shimokuzawa, Sagamihara, Kanagawa 229, Japan

(Received 2 August 1994)

Internal photoemission spectroscopy characteristics for a PtSi/*p*-type Si Schottky-barrier diode have been studied. The authors present a one-dimensional calculation of the internal photoemission spectroscopy for Schottky-barrier diodes, taking into account the effective barrier height and the position from the PtSi/*p*-type Si interface. The internal photoemission spectroscopy characteristics so calculated are then compared with the measured characteristics obtained for PtSi/*p*-type Si Schottky-barrier diodes under different PtSi thicknesses and applied voltage conditions. The hot hole escape depths in both PtSi and Si are then determined and the excitation energy effects are presented.

I. INTRODUCTION

Internal photoemission spectroscopy for Schottky-barrier diodes has been widely studied, mainly for the metal/*n*-type Si Schottky-barrier diode. Recently, hot-electron transport in the CoSi₂/*n*-type Si Schottky-barrier diode has been studied.¹ The hot-electron escape depth in the CoSi₂ has been deduced, through comparing a one-dimensional internal photoemission spectroscopy model with the measurement results. However, the internal photoemission spectroscopy model has poorly traced the measurement results.

The PtSi/*p*-type Si Schottky-barrier diode is one of the most attractive systems. The internal photoemission spectroscopy for the PtSi/*p*-type Si Schottky-barrier diode allows one to study the transport phenomena of photoexcited holes in metal and Si. The internal photoemission spectroscopy characteristics have been studied for PtSi/*p*-type Si Schottky-barrier diodes by Elabd and Kosonocky.² In the study, photoexcited holes were similarly treated with hot electrons, except that the total kinetic energy of the hole was measured from the metal (PtSi) Fermi level, while, conversely, that for the electron was measured from the bottom of the conduction band. However, the study was based on the wrong assumption that $\sqrt{h\nu/\Phi_b} \sim h\nu/\Phi_b$. For the hot hole in PtSi/*p*-type Si, it is obvious that the assumption of $\sqrt{0.7/0.2} \sim 0.7/0.2$ is wrong in the typical Schottky-barrier height of 0.2 eV and incident photon energy in the range from 0.2 to 0.7 eV.

It should also be noted that all studies concerning internal photoemission poorly address the problem of effective barrier position from the metal/Si interface in Si caused by the image force lowering effect (the Schottky effect).^{3,4} A precise study of hot hole transport in metals, based on internal photoemission spectroscopy, requires that one take into account the Schottky effect to calculate the photo response.

In this paper, the hot hole multireflection in the PtSi/*p*-type Si Schottky-barrier diode was studied using

the internal photoemission spectroscopy model, which first includes the image force lowering effect. The escape depths for holes in PtSi and Si are first reported by comparing with the internal photoemission spectroscopy model and the internal photoemission spectroscopy results for the various thicknesses and applied bias voltages for PtSi/*p*-type Si Schottky-barrier diode.

II. EXPERIMENT

PtSi Schottky-barrier diodes were fabricated on *p*-type silicon substrates. The silicon substrates were mirror polished on both sides, since they were back illuminated during internal photoemission spectroscopy measurements. A frame-shaped *n*-type diffused guard ring was first formed on the *p*-type silicon surface. The inside region of the guard ring, which was the diode effective area, was 300 μm square. The silicon surface was covered by SiO₂, and a square window was opened in the overlap to the guard ring. Immediately before being loaded into an ultrahigh vacuum (UHV) electron-gun evaporator, the wafers were dipped into diluted HF for 30 s, rinsed briefly in deionized water, and dried. Following a pumping down to 1×10^{-8} Pa, thin platinum films were deposited. The thicknesses were ranging between 1.5 and 15 nm. During the evaporation and successive 10 min, the wafers were kept at 620 K to form Pt silicide, PtSi. The 3- and 30-nm PtSi films were grown on the open region with polycrystal grains predominantly grown in PtSi($\bar{1}\bar{1}0$)||Si(001) orientation. Then nonreacted Pt, deposited on SiO₂, was removed by aquaregia. Finally, the PtSi surface was covered by a 1-μm-thick SiO₂ film.

The PtSi/*p*-type Si Schottky-barrier diodes were mounted in a nitrogen cryostat and then cooled down to 80 K. The internal photoemission spectroscopy characteristics were measured, using a standard blackbody light source with an optical chopper and several kinds of narrow-bandpass optical filters (NBPF's). The typical transmit window for the NBPF is 2–4% full wavelength half minimum (FWHM) to their center wavelengths. The

NBPF units were free from sideband transmittance. The measurements were carried out on diodes whose PtSi thicknesses were between 3 and 30 nm at reverse bias voltages ranging from 0 and 5 V. The infrared probe lights were irradiated from the mirror-polished Si back surface.

Temperature-dependent I - V characteristics for the 3-nm PtSi/ p -type Si Schottky-barrier diode were obtained with a temperature controlled cryostat in the from 80–150 K range. The effective Schottky-barrier height and barrier position measured from the PtSi/ p -type Si interface are deduced from the I - V data comparison with a potential calculation based on the thermionic emission theory, combined with the image force lowering effect, as shown in the following equation:

$$J = A^{**} T^2 \exp \left[\frac{q\Phi_b(V)}{kT} \right] \exp \left[\left[\frac{qV}{kT} \right] - 1 \right]. \quad (1)$$

Here $\Phi_b(V)$ is the effective Schottky-barrier height, which depends on the applied voltage due to the image force lowering effect. The other symbols are the same as those used conventionally.

In this study, the PtSi film was treated as a summation of $\Delta t = 0.1$ -nm thickness slices of the infrared light absorbent. The absorbance in the number x th slice from the Si interface, $\text{Abs}(h\nu, x)$, can be described by Eq. (2). The incident light ratio to the initial intensity at the x th slice and the absorption ratio are $\exp[-(x-1)\Delta ta(h\nu)]$ and $1 - \exp[-\Delta ta(h\nu)]$, respectively:

$$\text{Abs}(h\nu, x) = \{ \exp[-(x-1)\Delta ta(h\nu)] \} \times \{ 1 - \exp[-\Delta ta(h\nu)] \}. \quad (2)$$

The relationship between the measurement values and absorbance coefficient, $a(h\nu)$, is described by Eq. (3)

$$1 - [T(h\nu) + R(h\nu)] = 1 - \exp[-ta(h\nu)]. \quad (3)$$

Here $T(h\nu)$ and $R(h\nu)$ are the optical transmittance and reflectance for the PtSi film, respectively. The symbol t is the PtSi thickness. $\text{Abs}(h\nu, x)$ can be obtained by the $T(h\nu)$ and $R(h\nu)$ measurements by using Eqs. (2) and (3).

III. EXPERIMENTAL RESULTS

The results of the internal photoemission spectroscopy measurements are shown in Fig. 1. From Eq. (32) in Ref. 2, the slope and the intercept for the rising curve correspond to $A(h\nu)G(h\nu)$ and $\sqrt{\Phi_b}$, respectively. Here, $A(h\nu)$ and $G(h\nu)$ are optical absorbance and gain coefficient, respectively. The rising curve means that $A(h\nu)G(h\nu)$ depends on the incident infrared light energy $h\nu$. Due to the rising curve, the Schottky-barrier height Φ_b cannot be simply deduced.

The Schottky-barrier height and the barrier position from the PtSi/ p -type Si interface are deduced by the comparison between the I - V data and the calculation using the thermionic emission theory combined with the image force lowering effect. The results were summarized in Table I. The barrier height and position depend on the reverse bias voltage conditions.

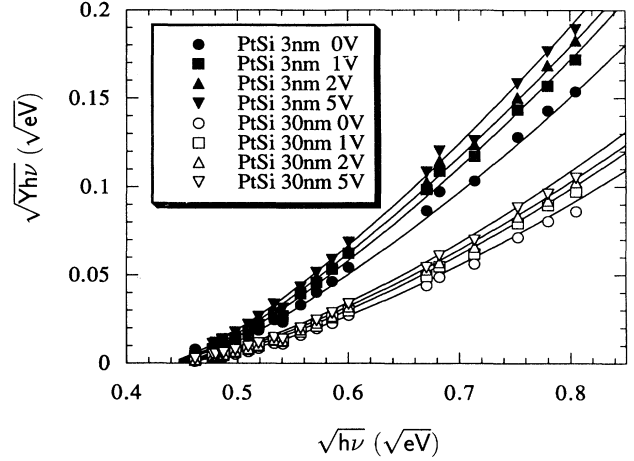


FIG. 1. Internal photoemission spectroscopy characteristics for PtSi/ p -type Si Schottky-barrier diodes. The x axis is the square root of the incident photon energy. The y axis is the square root of the product of the photo yield and incident photon energy. Closed and open symbols show the 3- and 30-nm PtSi film thicknesses, respectively. The circle symbols show the 0-V applied reverse bias voltages. The square, triangle, and inverted triangle symbols show 1-, 2-, and 5-V bias voltages, respectively. The solid lines are calculated curves using Eq. (11) (see text).

The absorbance characteristics in the thin (3 nm) and thick (30 nm) PtSi films are shown by Eqs. (4) and (5), respectively.

$$a(h\nu) = 1.721 \times 10^{-2} \times h\nu^2 - 2.276 \times 10^{-2} \times h\nu + 1.9784 \times 10^{-2} \quad (3\text{-nm PtSi film}), \quad (4)$$

$$a(h\nu) = 3.3 \times 10^{-2} \quad (30\text{-nm PtSi film}). \quad (5)$$

The absorbance $\text{Abs}(h\nu, x)$ of the thin film (3 nm) depends closely on the incident photon energy. On the other hand, that for the thick film (30 nm) does not show much dependence. The same tendency has been reported by Mooney.⁵

IV. DISCUSSION

A. Consideration for bend curves

There are several causes for the rising curve in Fig. 1; (i) the hot hole tunneling through the barrier,⁶ (ii) the thermally excited carrier effect by phonons,⁷ (iii) the incident energy dependence of the optical absorbance,² (iv) the hot hole multireflection effect in the metal electrode,²

TABLE I. Effective Schottky-barrier height and the barrier peak position deduced from the I - V characteristics.

Reverse bias voltage (V)	Φ_b (eV)	d (nm)
0	0.194	9.67
1	0.190	5.71
2	0.189	5.00
5	0.185	3.92

etc.

First, it can be concluded that the tunneling effect is small enough to be ignored under these experimental conditions. The depletion around the top of the barrier is thick enough to completely obstruct the hole injection, because the boron-doping concentration is as small as $2.5 \times 10^{14} \text{ cm}^{-3}$.

Next, we discuss the thermally excited carrier effect on internal photoemission spectroscopy. Due to the thermally excited carrier effect, experimental points in Fig. 1 are expected to deviate from the line at a low energy around the Schottky-barrier height.⁴ However, the effect should be insignificant at a high photon energy range. Therefore, on the assumption that the thermally excited carrier effect is a predominant factor for the deviation, the Schottky-barrier height for the 3-nm PtSi thickness diode at the 0-V condition can be obtained as 0.29 (eV), which was deduced from fitting to the data points at $\sqrt{h\nu}=0.67\text{--}0.72$. However, in Fig. 1, the diode obviously detected photons whose energies ($h\nu$) are around 0.21 eV ($\sqrt{h\nu}=0.458$). The 0.08-eV energy difference, which is obtained by subtracting 0.21 from 0.29 eV, is much larger than the maximum thermal excited phonon energy ($3kT$) of 0.02 (eV) of 80 K. Here k and T are Boltzmann's constant and operation temperature, respectively. Thus the thermally excited carrier effect is not a predominant factor for determining the rising curve characteristics. However, the effect might have a minor effect on the rising curve characteristics. Therefore, the thermally excited carrier effect is included in the internal photoemission spectroscopy model, proposed in Sec. IV B.

The incident photon energy dependencies on the absorption were already shown in Eqs. (4) and (5) for 3- and 30-nm PtSi films, respectively. Since the 30-nm PtSi was constant, the rising curve for 30 nm in Fig. 1 cannot be explained by the absorption characteristics. The absorbance characteristics are taken into account in the internal photoemission spectroscopy model to strictly compare to data sets.

Finally, we discuss the hot hole multireflection effect, taking into account the effective barrier position from the PtSi/*p*-type Si interface in Si. The effective barrier position is separate from the PtSi/*p*-type Si interface, due to the image force lowering effect. Figure 2 shows the potential diagram for the PtSi/*p*-type Si Schottky-barrier diode and the photoexcited hole behavior. The effective barrier height and the barrier peak position, measured from the PtSi/*p*-type Si interface, are labeled Φ_b and d , respectively. In Sec. IV B, behaviors for photoexcited holes are discussed as predominant factors in the internal photoemission spectroscopy model.

B. Photoinjection model for a *p*-type Schottky-barrier photodiode

The following traces the behavior for a hot hole, generated at position x in the slice width of Δt in Fig. 2.

First, the incident photon is absorbed in the PtSi film to generate a photoexcited hole. The absorbances $\text{Abs}(h\nu, x)$, are determined according to Eqs. (2), (4), and (5). The escape probability is related to the probability of

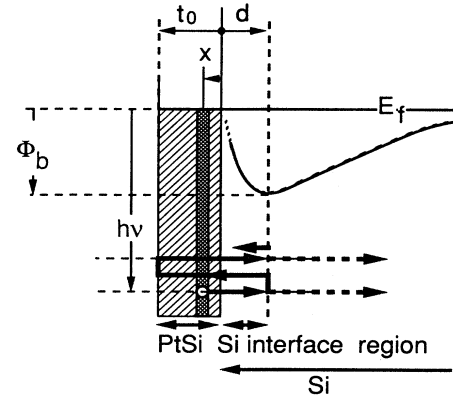


FIG. 2. Potential diagram for the PtSi/*p*-type Si Schottky-barrier diode. The photoexcited hole behavior is indicated.

the hot hole maintaining an energy higher than the barrier energy, until it reaches the barrier position d in Fig. 2. We assume that this escape probability can be described by an inelastic escape depth L , i.e., as an exponentially decreasing function of the distance between the hot hole creation position and the barrier.¹ In the case of a thin PtSi film and shallow effective barrier position, the hot hole maintains an energy higher than the barrier energy after multireflection at the effective barrier position and the SiO_2/PtSi interface. The ratio of the arrival hole number N , excluding the holes reflected at the effective barrier position, to the total generated hole number N_0 at the x position, $\text{escd}(x, 1)$, is described as follows:

$$\text{escd}(x, 1) = \frac{N}{N_0} = \frac{1}{2} \left[\exp \left\{ - \left[\frac{x}{L_{\text{PtSi}}} + \frac{d}{L_{\text{Si}}} \right] \right\} + \exp \left\{ - \left[\frac{2t - x}{L_{\text{PtSi}}} + \frac{d}{L_{\text{Si}}} \right] \right\} \right]. \quad (6)$$

Here, the number 1 in $\text{escd}(x, 1)$ means the condition before reflection at the effective barrier position. The function $\text{escd}(x, 1)$ includes the hot hole reflected one time at the SiO_2/PtSi interface. L_{PtSi} and L_{Si} are inelastic escape depths in PtSi film and the Si interface region, respectively. The Si interface region means the Si region between the PtSi/*p*-type Si interface and the effective Schottky-barrier position. It is first defined as the escape depth in the Si interface region, L_{Si} . In Eq. (6), t and d are the PtSi film thickness and the barrier position measured from the PtSi/*p*-type Si interface, respectively.

The basic reason for the variation in quantum yield with photon energy for energies above the threshold is that a hole can escape only if it has a momentum component normal to the Schottky barrier at the barrier position.⁸ Thus, the internal quantum yield, considering the hole generated at the x position, $Y_{\text{int}}[h\nu, x, 1]$, is as described in Eq. (7):

$$Y_{\text{int}}[h\nu, x, 1] = \frac{1}{h\nu} \int_{\Phi_b}^{h\nu} \text{escd}(x, 1) * \left[1 - \left(\frac{\Phi_b}{E} \right)^{1/2} \right] dE. \quad (7)$$

Here Φb and $h\nu$ are the effective Schottky-barrier height and incident photon energy, respectively. The meanings for x and 1 in $Y_{\text{int}}[h\nu, x, 1]$ are the same as in $\text{escd}[x, 1]$.

In a thin PtSi film, it is known that the escape probability for a photoexcited hole increases by a multireflecting effect between the PtSi surface and Schottky-barrier position.² The following equation is revised from Eq. (6), by including the multireflecting effect:

$$\begin{aligned} \text{escd}(x, n) = & \frac{1}{2} \left[\exp \left\{ -2(n-1) \left[\frac{x}{L_{\text{PtSi}}} + \frac{d}{L_{\text{Si}}} \right] \right\} \right. \\ & \left. + \exp \left\{ - \left[\frac{2t-x}{L_{\text{PtSi}}} + \frac{d}{L_{\text{Si}}} \right] \right\} \right] \\ & \times \left\{ \prod_{k=1}^n \left[\left(\frac{\Phi b}{E} \right)^{1/2} \right]^{k-1} \right\}. \end{aligned} \quad (8)$$

The meaning of $\text{escd}(x, n)$ is the same as $\text{escd}(x, 1)$ except for the arrival hole, which maintains an energy higher than the barrier energy after $(n-1)$ times multireflection. Here the product term in the integral is for consideration with the remaining part, after the last reflection at the barrier position.

$Y_{\text{int}}[h\nu, x, n]$ is the same as the $Y_{\text{int}}[h\nu, x, 1]$, except for the $(n-1)$ multireflection. The quantum yield for the hole generated at the x position is then described, using Eq. (9), as

$$Y_{\text{int}}[x, n] = \frac{1}{h\nu} \int_{\Phi b}^{h\nu} \left\{ \text{escd}(x, n) * \left[1 - \left(\frac{\Phi b}{E} \right)^{1/2} \right] dE \right\}. \quad (9)$$

The total quantum yield, $Y_{\text{total}}[h\nu]$, is described according to Eq. (10),

$$Y_{\text{total}}[h\nu] = \sum_{x=1}^{t/\Delta t} \left[\text{Abs}(x, n) \sum_{n=1}^{+\infty} (Y_{\text{int}}[h\nu, x, n]) \right]. \quad (10)$$

Finally, the quantum yield, $Y_{\text{total}}^{\text{phonon}}[h\nu]$, is described according to Eq. (11), considering the phonon-excited carrier effect:

$$Y_{\text{total}}^{\text{phonon}}[h\nu] = \int_{-\infty}^{+\infty} \frac{1}{1 + \exp \left[\frac{-\Delta E}{kT} \right]} Y_{\text{total}}[h\nu] d\Delta E. \quad (11)$$

Here T and ΔE are the diode operation temperature and the deviation energy from the metal Fermi level, respectively.

C. Comparison between calculated and measured quantum yields

The quantum yields are calculated using Eq. (11). In the calculation, free parameters are escape depths in the PtSi film, L_{PtSi} , and the Si interface region, L_{Si} . The Schottky-barrier heights and the positions are regarded as the same values as indicated in Table I, which were deduced by the temperature dependence of I - V measure-

ments. We assumed that the Schottky-barrier height is independent of the PtSi film thickness.

The data set for the quantum yields obtained by using the internal photoemission spectroscopy model is compared to the measured data set, as shown in Fig. 1. Note that the calculation curves closely trace the data points. The comparing process determines the escape depths in the PtSi film and the Si interface region. The obtained escape depths are shown in Fig. 3. A hot hole, excited by a high-energy photon, is expected to maintain an energy above the barrier height for a long travel distance. The escape depths increase with the incident photon energy in Fig. 3, which is in good agreement with what was expected.

As far as we know, this is the first report concerning hole escape depth. Hence it is not possible to compare the deduced escape depths with other data sets. Here we discuss the reliability of the escape depths. First, the predominant factor for the hot hole escape depth is the phonon (lattice) scattering in the measured energy range. In Fig. 3, the determined escape depth for Si is larger than that for PtSi. This is in good agreement with the fact that the Si crystal is a single crystal. Conversely, PtSi is a polycrystal. Next, the estimated hole escape depths are compared with a reported electron escape depth in a similar energy range.¹ The electron escape depth was reported to be in the range between 7 and 10 nm for the photon energy range between 0.75 and 1 eV. The electron escape depth is on the same order as the hole escape depth, as shown in Fig. 3.

The escape depths in PtSi are approximately the same values for all applied voltages. Those in Si are the same for all applied voltages except 0 V. These correspondences suggest that the escape depths can be determined as these material original characteristics. The deviation in the escape depth for 0 V from other applied voltages in Si may be caused by the fact that the hot hole is reflected at a position between the interface and the effective barrier position. This study does not consider the energy

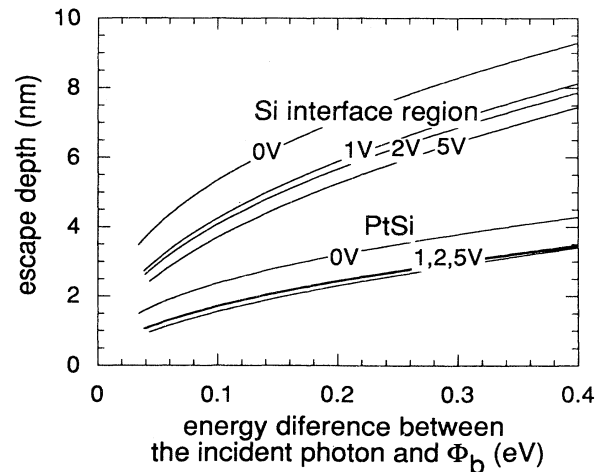


FIG. 3. Photoexcited hole escape depths. The x axis indicates the difference between the incident photon energy and Schottky-barrier height. The y axis indicates the escape depth.

distribution for the hot hole. The energy distribution effect should approach the reflection position to the interface. This effect may be remarkable in the flat potential around the effective barrier position for Si 0-V bias voltage.

Recently, the hot hole effect has been examined in a BEEM (ballistic-electron-emission microscopy) study.⁹ The hot hole could not be observed directly in the BEEM study. However, the hot hole behavior is expected to be indicated using BEEM.

V. CONCLUSION

Internal photoemission spectroscopy characteristics for PtSi/*p*-type Si Schottky-barrier diodes were precisely

studied, taking into account the image force lowering effect. The internal photoemission spectroscopy for the PtSi/*p*-type Si Schottky-barrier diode allows us to make a study of the transport of photoexcited holes in PtSi and Si. The quantum yields so calculated are then compared with the measured ones obtained on PtSi/*p*-type Si Schottky-barrier diodes with different PtSi thicknesses and applied voltage conditions. The hot hole escape depths in both PtSi and Si are determined.

ACKNOWLEDGMENTS

The authors would like to thank H. Utsumi and K. Masubuchi for their assistance.

¹J. Y. Duboz and P. A. Badoz, *Phys. Rev. B* **44**, 8061 (1991).

²H. Elabd and W. F. Kosonocky, *RCA Rev.* **43**, 569 (1982).

³S. M. Sze, C. R. Crowell, and D. Kahng, *J. Appl. Phys.* **35**, 2534 (1964).

⁴E. H. Rhoderick, *Metal-Semiconductor Contacts* (Clarendon, Oxford, 1978).

⁵J. M. Mooney, *J. Appl. Phys.* **64**, 4664 (1988).

⁶J.-C. Wu and J.-T. Lue, *Solid State Electron.* **30**, 97 (1987).

⁷A. M. Goodman, *J. Appl. Phys.* **35**, 573 (1964).

⁸R. K. Willardson and A. C. Beer, *Semiconductor and Semimetals* (Academic, New York, 1970), Vol. 6, Chap. 2.

⁹P. Niedermann and L. Quattropani, *Phys. Rev. B* **48**, 8833 (1993).